NGU Report 2011.024

Safe Operations of Subsea Systems (SOSS) – sea bed data from the physical test site in the Trondheimsfjord

Norges geologiske undersøkelse
Postboks 6315 Sluppen
7491 TRONDHEIM
Tlf. 73 90 40 00
Telefaks 73 92 16 20

REPORT

Report no.: 2011.024 | ISSN 0800-3416 | Grading: Open

Title:
Safe Operations of Subsea Systems (SOSS) - sea bed data from the physical test site in the Trondheimsfjord

Authors:
Oddvar Longva

Client:
Sintef Fisheries and Aquaculture Ltd.

County:
Norway

Commune:
Trondheim

Map-sheet name (M=1:250.000)
Trondheim

Map-sheet no. and -name (M=1:50.000)
1621.4 Trondheim

Deposit name and grid-reference:

Number of pages: 29 Price (NOK): 65,-
Map enclosures: 0

Fieldwork carried out:
28.- 29.09.2010

Date of report:
18.02.2011

Project no.:
328300

Person responsible:
Reidulv Bøe

Summary:
A shallow water area east of Trondheim harbour in the Trondheimsfjord has been used as test site to study the impact of towed bottom gear on seafloor sediments in the frame of the SOSS project (Safe Operations of Subsea Systems). This report presents detailed bathymetry, acoustic reflectivity and grain size analyses of seafloor sediments in the test area.

SINTEF Fisheries and Aquaculture, in cooperation with Marine Scotland, performed towing tests with a sledge loaded with instruments in the period 31th August 2010 - 6th September 2010. The tests were performed from the NTNU vessel R/V Gunnerus. In September 2010 NGU mapped the test area with a GeoSwath 250 kHz interferometric sonar, collected high resolution sub-bottom profiler data with a Kongsberg S40 Topas parametric source, and aquired grab samples and Niemistöe cores at four locations. The survey was done with the NGU vessel FF Seisma.

The seabed in the test area comprises an upper sandy gravelly mud layer 5-10 cm thick resting on softer and more fine-grained muds. Comparisons of bathymetric datasets from 2004 and 2010 show that the test tows did not make significant scours into the sea bed.

The high content of coarse silt and sand makes the soil dilatant. The seabed will have a firm behavior if it is hit by a falling object like a gravity corer, while vibrations will cause objects to sink into the seabed. This infers further that an object that lies on the seabed vibrating or rocking, e.g. due to drag in a line may sink into the seabed. The sledge that was towed at constant speed over the seabed caused only minor influence on the seabed.

Keywords: Swath bathymetry	Acoustic reflectivity	Coring
Seafloor sediments	Grain size distribution	Seismic
Stratigraphy	Subsea operations	Safety

CONTENTS

FIGURES

Figure 1. Location of the test area (black rectangle). Dates for individual lines are given in the legend.

Figure 2. The same area mapped with GeoSwath 250 kHz interferometric sonar in 2004 and 2010. The 2010 data are better processed than the older dataset, but the grooves in the sea bed are the same - marked with arrows - in both datasets. The tow tests have not made visible imprints on the sea bed.

Figure 3. Bathymetry with 2 m contour intervals and interferometric sonar backscatter draped on the terrain model. The backscatter map shows acoustic energy reflected from the sea bed during depth sounding. Dark colour shows relative hard bottom - light colour soft bottom. The thin yellow lines represent survey lines with GeoSwath Interferometric Sonar and Topas sub-bottom profiler. The other lines represent test tow lines reconstructed from Olex print screens taken during the tests. The coloured dots are vessel positions taken from these screen dumps. Sample locations are indicated with red and green circles and the last number of the sample identification (1 is synonymous with P1009001 etc.). Sections of three seismic lines crossing over the sample locations are shown in Fig. 4.

Figure 4. High resolution seismic lines from the Topas sub-bottom profiler. Line NGU 1009013 is shown in full length, while NGU 1009004 and NGU 1009008 cover the stretches over the core locations. The distance between horizontal grid lines is approximately 90 m and c. 15 m between vertical grid lines. The sub-bottom reflections represent acoustic layering in the sediment indicating variations in sediment properties. The colour of the seabed reflection indicates relative hardness of the top sediments. Strong red reflection is "hard" and faint blue is "soft".

Figure 5. Core P1009006 was split in 8 subsamples. Grain size distribution is shown as volume percentages, while median is the grain size at 50 volume percent. Clay comprises the fraction smaller than 2 µm, silt is 2-63 µm, sand 63-200 µm and gravel larger than 200 µm. The complete analytical report is shown in Appendix 1.

TABLES

Table 1. Grab samples and cores.

Table 2. Sample data. The median is from the upper 5 cm of the Niemistoe cores and the upper 5-10 cm for the grab samples.

APPENDIX

Analyserapport 2010.0371

1. INTRODUCTION

Recent history has shown that the handling of subsea systems involves significant operational risk. Fishermen are exposed to higher risk levels than most other occupational groups in Norway. Handling of subsea systems are often characterized by a combination of heavy loads, rough environmental conditions and complex interplay between the vessel stability and the forces from the subsea system. Accomplishing the operations with acceptable levels of safety may pose big demands on continuously analyzing the operational risk of the seamen. The SOSS project (Safe Operations of Subsea Systems) is financed by the Norwegian Research Council to study this. The aim of the project is to make reliable models in combination with measurements and produce decision support systems able to provide on-line information to the operator about important subsea system states, making him able to predict and avoid dangerous situations.

Particular challenges are the modeling of anchor chains and towing wires, environmental loads, fishing gear and all devices that have interaction with the seabed. The latter is a major activity in the SOSS project, and considerable effort is put into studying forces acting from the sediments to the subsea systems.

A shallow water area east of Trondheim harbour in the Trondheimsfjord (Fig. 1) was used as a test site to study the impact of towed bottom gear on seafloor sediments. This report presents detailed bathymetry, acoustic reflectivity and grain size analyses of seafloor sediments in the test area.

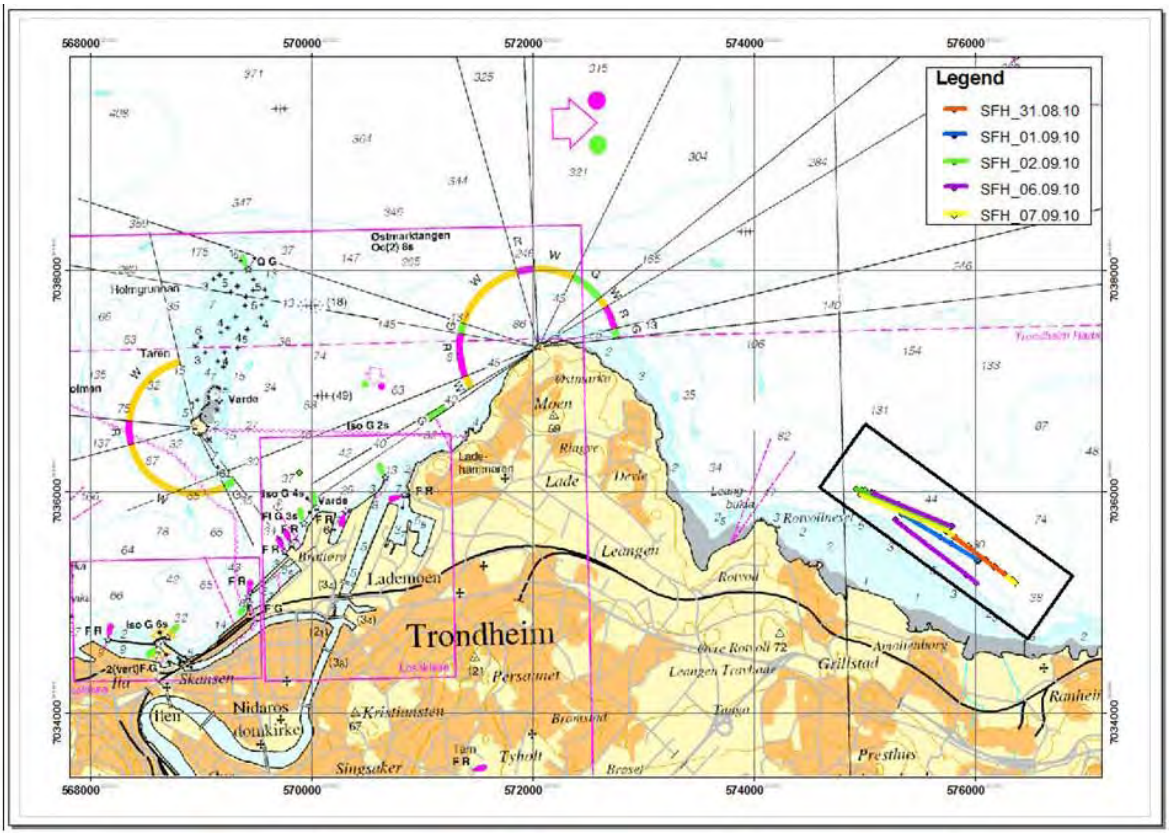

Figure 1. Location of the test area (black rectangele). Dates for individual lines are given in the legend.

2. METHODS

SINTEF Fisheries and Aquaculture, in cooperation with Marine Scotland, performed towing tests with a sledge loaded with instruments in the period 31th August 2010 - 6th September 2010. The tests were performed from the NTNU vessel R/V Gunnerus. In September 2010 NGU mapped the test area with a GeoSwath 250 kHz interferometric sonar, collected high resolution sub-bottom profiler data with a Kongsberg S40 Topas parametric source, and aquired grab samples and Niemistoe cores at four locations. The survey was done with the NGU vessel FF Seisma. Crew onboard Seisma were Eilif Danielsen, Oddbjørn Totland and John Anders Dahl.

2.1 Swath bathymetry

The interferometric sonar was used to map water depths over the test area. The same area was mapped in 2004 and the datasets were compared to check for morphological changes. The sonar produces high-resolution bathymetric and backscatter data for water depth range 0-80 m. The sonar has two transducers mounted on a V-plate at 30 degrees to vertical that alternately collect the signal. A sound velocity probe, a single beam echosounder, and a motion reference unit (MRU) for measuring heave, pitch and roll are also fitted to the V-plate. Each transducer is equipped with one transmitter and four phase differencing interferometric and sidescan receivers. All four receivers record time series of the returning echo from the ensonified area. The relative phase and phase delay between the four receivers is used for determining the angle of the returning echo, which combined with the elapsed time, permits calculation of the distance to the scattering location at the seabed. The amplitude of the signal provides backscatter information, which is a measure of the relative texture and hardness of the seabed. The across track sampling density of the GeoSwath system is 1.5 cm, and vertical resolution is estimated to be $\leq$ 2 cm (GeoAcoustics, 2004). Vessel speed during the profiling was 4 knots, which with a ping rate of ca. 6 pings/s gives along-track resolution of ca. 65 cm.

Line spacing during the 2010 sonar survey was c 50 m, with closer distance in the shallowest areas. In order to correct for sound velocity variations and refractive effects in the water column due to temperature and salinity differences, two types of sound velocity measurements were undertaken. Valeport Mini SVS sound velocity probe, mounted on the sonar head, provided a continuous, real-time sound velocity record during acquisition. Sound velocity profiles with 25 cm vertical resolution from the surface down to the seafloor were obtained several times every day at different parts of the survey area using a Valeport 650 sound velocity profiler. Sub-meter accuracy for horizontal positioning was accomplished by a Trimble differential GPS system. A gyrocompass, connected to the DGPS was used to obtain heading data. The sonar data were filtered for water column noise below the transducer during acquisition. All data processing operations were done with GeoSwath software including: (i) filtering for outliers; (ii) calibration for sonar parameters; (iii) sound velocity corrections; (iv) tidal corrections; (v) navigation check; and (vi) gridding with 1 m horizontal bins. The sea level time series from Trondheim harbor, measured by the Norwegian Mapping Authority, were used for the tidal corrections. The study area is located ca. 6 km from Trondheim harbour and it is assumed that the difference in tidal wave propagation is negligible across such a short distance.

2.2 Parametric sub-bottom profiler (Topas)

High-frequency shallow seismic data were acquired using a parametric sub-bottom profiler (Topas PS 40 from Kongsberg) simultaneously with the acquisition of sonar data. Positions of seismic lines (ship tracks) that run through the area are shown on Fig. 3. Topas uses a parametric acoustic source that forms a 5 degrees wide beam. The profiler was operated in the chirp mode with primary frequencies of 36-39 and 41-44 kHz, and chirp length of 10 ms. The returning signal was sampled within the frequency range of 2-8 kHz with the median frequency of 5 kHz. Such sampling frequency provides a vertical resolution of ca. 0.2 ms (ca. 15 cm). Examples of the seismic is shown in Fig. 4.

2.3 Coring

Four locations were sampled with a 30 x 30 cm wide box corer and a Niemistöe gravity corer with 50 cm core liner and a weight of c. 40 kg. The cores were located close to or at SFH tow lines and in a cross over the area to get differences in sediment compositions along shore and from shallow to deeper water (Fig. 3). The box corer came up with samples at all four locations (see Table 1). It was emptied on deck and bulk samples of the upper 10 cm were stored for grain size analyses. The Niemistöe corer had problems to penetrate the firm upper sea floor sediments and at 3 out of 4 locations several trials were carried out. In two locations we got no sample (Table 1).

Table 1. Grab samples and cores.

Sample	N_utm32	E_utm32	Waterdepth	Corer	Core length	Trials
P1009001	7035840	575480	32	Grab	15	1
P1009002	7035670	575670	27	Grab	10	1
P1009003	7035772	575762	37	Grab	12	1
P1009004	7035552	575844	33	Grab	15	1
P1009005	7035538	575568	15	Grab	8	1
P1009006	7035532	575561	15	Niemistoe	41	1
P1009007	7035813	575494	33	Niemistoe	-	3
P1009008	7035675	575672	28	Niemistoe	3	2
P1009009	7035761	575740	36	Niemistoe	-	2
P1009010	7035536	575823	31	Niemistoe	10	2

2.4 Grain size analyses

The Niemistoe cores were stored upright. Later they were extruded from the core liner and split into 5 cm long cylinders at the NGU laboratory. These and the grab samples were wet sieved and fractions weighed. The distribution of fractions smaller than 63 µm were analyzed in a Coulter Ls 200. The coulter counter has a tendency to underestimate the clay content with many percentages compared to analyses with pipette or hydrometer. Laboratory Report 2010.0371 is enclosed as Appendix 1.

3. RESULTS

3.1 Tool marks on the sea floor

Shadow relief images based on the surveys in 2004 and 2010 were compared to see if the towed sledge had made significant imprints into the seafloor sediments.

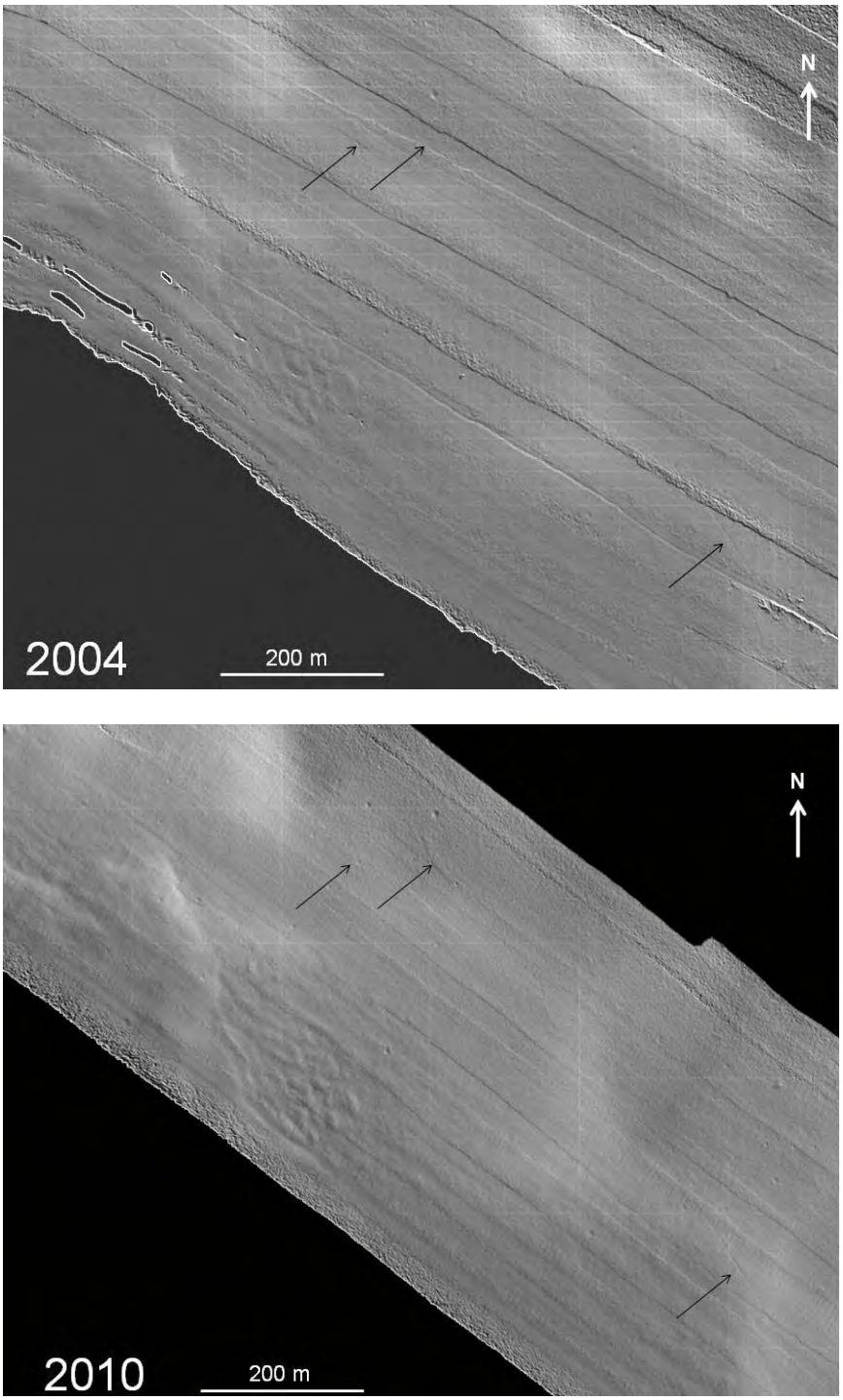

Figure 2. The same area mapped with GeoSwath 250 kHz interferometric sonar in 2004 and 2010. The 2010 data are better processed than the older dataset, but the grooves in the sea bed are the same - marked with arrows - in both datasets. The tow tests have not made visible imprints on the sea bed.

Scour marks c. 10 cm deep that are seen on both images and are hence older than the trials in September 2010. Along the reconstructed tow lines from the tests, no lineaments can be seen on the seafloor indicating that the sledge slid on top of the sediments without making significant imprints, if any. This implies that the seabed is quite firm.

3.2 Sea floor sediments

The top reflector on the seismic registrations indicate a hard top layer. This impression is supported by the fact that the test tows of a sledge on the sea floor has made no visible scours on the sea bed.

The seismic reflectors are tilted in relation to the sea floor and crop out on the surface. This means that the original sediment stack has been eroded and that the top layer is a erosion lag which is coarser than the sediments beneath.

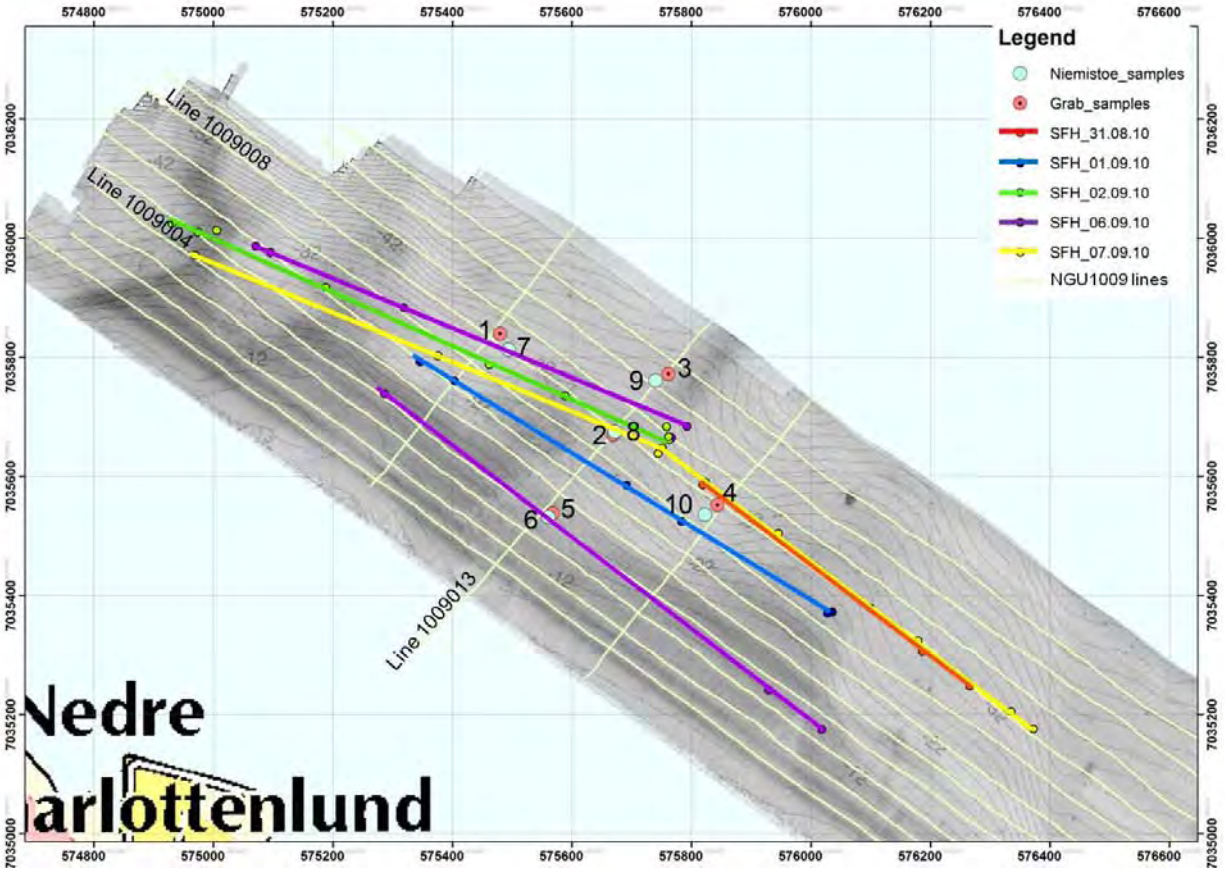

Figure 3. Bathymetry with 2 m contour intervals and interferometric sonar backscatter draped on the terrain model. The backscatter map shows acoustic energy reflected from the sea bed during depth sounding. Dark colour shows relative hard bottom - light colour soft bottom. The thin yellow lines represent survey lines with GeoSwath Interferometric Sonar and Topas sub-bottom profiler. The other lines represent test tow lines reconstructed from Olex print screens taken during the tests. The coloured dots are vessel positions taken from these screen dumps. Sample locations are indicated with red and green circles and the last number of the sample identification (1 is synonymous with P1009001 etc.). Sections of three seismic lines crossing over the sample locations are shown in Fig. 4.

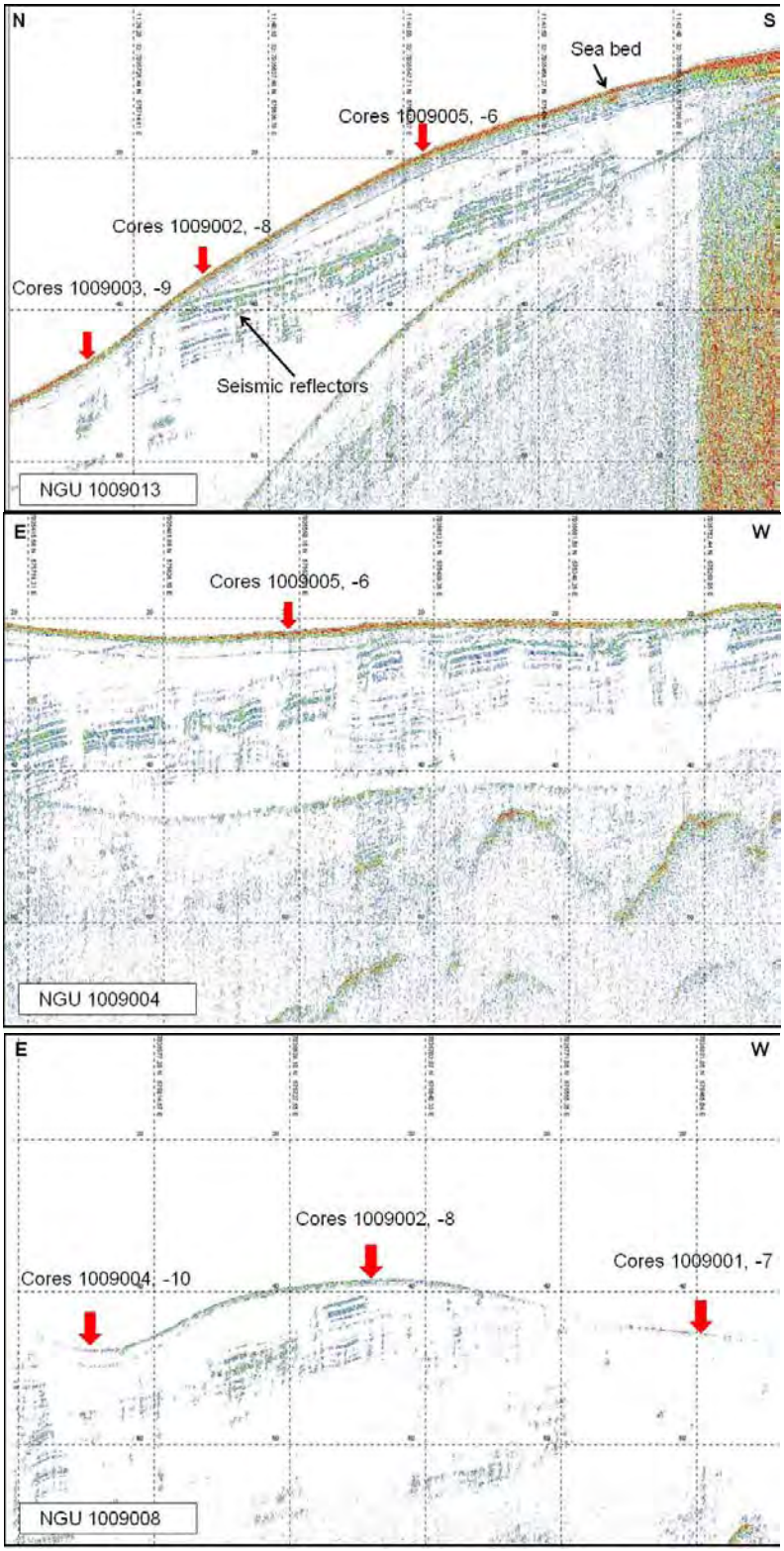

Figure 4. High resolution seismic lines from the Topas sub-bottom profiler. Line NGU 1009013 is shown in full length, while NGU 1009004 and NGU 1009008 cover the stretches over the core locations. The distance between horizontal grid lines is approximately 90 m and c. 15 m between vertical grid lines. The sub-bottom reflections represent acoustic layering in the sediment indicating variations in sediment properties. The colour of the seabed reflection indicates relative hardness of the top sediments. Strong red reflection is "hard" and faint blue is "soft".

One of the cores, P1009006, penetrated the top layer and a c. 40 cm long core was recovered. The core and grain size distribution downcore is shown in Fig. 5.

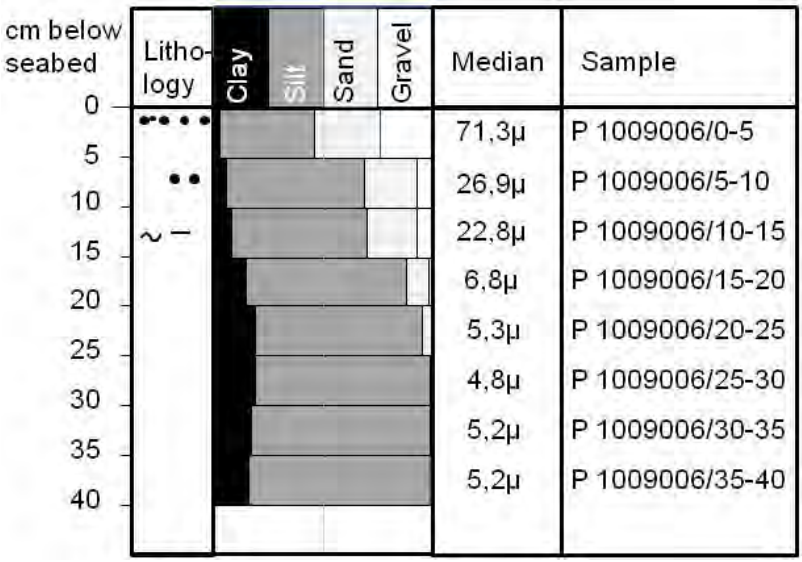

Figure 5. Core P1009006 was split in 8 subsamples. Grain size distribution is shown as volume percentages, while median is the grain size at 50 volume percent. Clay comprises the fraction smaller than 2 µm*, silt is 2-63* µm*, sand 63-200* µm *and gravel larger than 200* µm*. The complete analytical report is shown in Appendix 1.*

The grain size distribution shows that the upper 5 cm of the core is coarser than the sediments below. The samples down to 15 cm have more than 10% sand, while below that depth more than 90% is silt and clay. The sediments are originally glaciomarine, fine grained muds like those we see in the lower samples of the core and from the seismic signature seen in Fig. 4. However, current and wave action has eroded the seabed and winnowed the finest particles from the surface. Burrowing animals live in the upper 15-20 cm of the seabed. These animals bring fine sediments to the surface where they are washed by currents and wave action and they mix sand from the seabed into the sediments. The surface layer mainly comprises coarse silt and fine sand but also some gravel clasts and shell fragments.

Table 2. Sample data. The median is from the upper 5 cm of the Niemistöe cores and the upper 5-10 cm for the grab samples.

Sample	N_utm32	E_utm32	Water depth	Corer	Core length cm	Median µ
P1009005	7035538	575568	15	Grab	8	58
P1009006	7035532	575561	15	Niemistoe	41	71,3
P1009002	7035670	575670	27	Grab	10	53,6
P1009008	7035675	575672	28	Niemistoe	3	49,5
P1009004	7035552	575844	33	Grab	15	37,1
P1009010	7035536	575823	31	Niemistoe	10	39,7
P1009001	7035840	575480	32	Grab	15	41,4
P1009007	7035813	575494	33	Niemistoe	-	-
P1009003	7035772	575762	37	Grab	12	43,4
P1009009	7035761	575740	36	Niemistoe	-	-

Table 2 shows the median (grain size fraction at 50% volume) of the seabed samples. The grab samples are generally somewhat finer than the top 5 cm of the corresponding Niemistoe core. This can be explained by the sampling method as the grab samples are bulk samples and may include finer material below the coarsest top layer. The backscatter strength shown as intensity in grey colours in Fig. 3 weakens towards deeper water and is stronger over ridges than in depressions. This corresponds very well with the grain size analyses presented in Table 2.

The high content of coarse silt and sand makes the soil dilatant. The seabed will have a firm behavior if it is hit by a falling object like a gravity corer, while vibrations will cause objects to sink into the seabed. This infers further that an object that lies on the seabed vibrating or rocking, e.g. due to drag in a line may sink into the seabed. The sledge that was towed at constant speed over the seabed caused only minor influence on the seabed.

4. CONCLUSIONS

The seabed in the test area comprises an upper sandy gravelly mud layer 5-10 cm thick resting on softer and more fine grained muds. Comparisons of bathymetric datasets from 2004 and 2010 show that the test tows did not make any significant scours into the sea bed. The high content of coarse silt and sand makes the soil dilatant. The seabed will have a firm behavior if it is hit by a falling object like a gravity corer, while vibrations will cause objects to sink into the seabed. This infers further that an object that lies on the seabed vibrating or rocking, e.g. due to drag in a line may sink into the seabed. The sledge that was towed at constant speed over the seabed caused only minor influence on the seabed.

APPENDIX 1

Analyserapport 2010.0371

NGU
Norges geologiske undersøkelse
7491 TRONDHEIM
Tlf.: 73 90 40 00
Telefaks: 73 92 16 20

Kornfordelingsanalyser: Coulter laser partikkelteller
GEOLOGISK MATERIALE
Analysekontrakt nr.:2010.0371

INSTRUMENT: **Coulter LS 200**

METODE: **Metodeoppsettet er beskrevet i NGU-SD 5.11: Kornfordelingsanalyser: Coulter laser partikkelteller.**

Kornfordelingsbestemmelse basert på laserdiffraksjon. Laserlys brytes i ulike vinkler avhengig av størrelsen på partiklene, og registreres så av en rekke detektorer. De registrerte vinklene tilsvarer gitte partikkelstørrelser, og antall partikler er relatert til den intensiteten som den korresponderende detektoren registrerer. Kornfordelingen bestemmes således på volum-basis, med antagelse om ens tetthet på materialet vil kumulativ volum% være identisk med kumulativ masse%. Beregning på volum/masse-basis er basert på antagelse om sfæriske partikler.

MÅLEOMRÅDE : **0.4 µm - 2000 mm**

NB ! Metoden normaliserer alle data i måleområdet til sum 100 % (kumulativ %).
Måleområdet går kun ned til 0.4 µm og dette settes som nullpunkt mhp. kumulativ %.
Prøvene kan derfor inneholde materiale finere enn 0.4 µm.

ANALYSEUSIKKERHET: **± 10 % [kumulativ masse(volum) %]** *Usikkerheten er oppgitt med dekningsfaktor 2, tilsvarende et konfidensintervall på 95 %*

Bestemmelse av usikkerhet er basert på sammenligning av oppnådde resultater med sertifikatverdier for kvartsstandard BCR-131, samt presisjonsdata.
MERK! Metoden tar utgangspunkt i antagelse om sfæriske partikler. For prøver som avviker fra dette kan usikkerheten være større.

PRESISJON: **Det analyseres rutinemessig kontrollprøver som føres i kontrolldiagram (X-diagram). Disse kan forevises om ønskelig.**

FORBEHANDLING: **Ingen**

ANTALL PRØVER: **16**

ANMERKNINGER: Data for fraksjoner >2000 µm er fremkommet ved gravimetriske bestemmelser.

Gjengivelse av analysedata skal skje på en slik måte at meningsinnholdet i rapporten ikke endres.

Ferdig analysert	9-des-10	Wieslawa Koziel
	Dato	OPERATØR

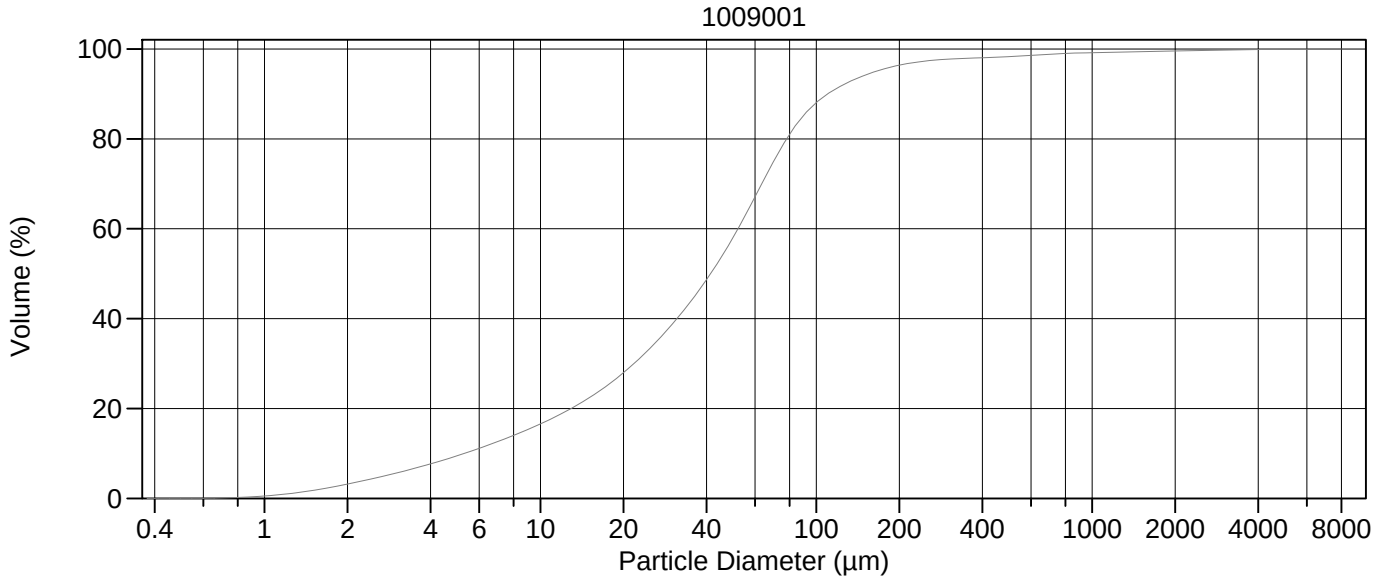

Volume Statistics (Arithmetic) 1a.$02

Calculations from 0.375 µm to 8000 µm

Volume	100.0%		
Mean:	77.60 µm	95% Conf. Limits:	0-616.9 µm
Median:	41.42 µm	S.D.:	275.1 µm
D(3,2):	12.94 µm	Variance:	75704 µm^2
Mean/Median Ratio:	1.874	C.V.:	355%
Mode:	60.52 µm	Skewness:	13.86 Right skewed
d_{10}:	5.300 µm	Kurtosis:	235.3 Leptokurtic
d_{50}:	41.42 µm		
d_{90}:	109.9 µm		
Specific Surf. Area	4636 cm^2/ml		

% <	10	25	50	75	90
Size µm	5.300	17.35	41.42	70.01	109.9

1a.$02

Particle Diameter µm	Volume % <	Particle Diameter µm	Volume % <
1.000	0.53	500.0	98.3
2.000	3.19	1000	99.2
5.000	9.50	2000	99.6
10.00	16.6	4000	99.9
15.00	22.3	8000	100
20.00	28.0		
50.00	58.1		
60.00	67.1		
63.00	69.7		
70.00	75.0		
75.00	78.2		
90.00	85.2		
125.0	92.0		
200.0	96.4		
250.0	97.3		
400.0	98.1		

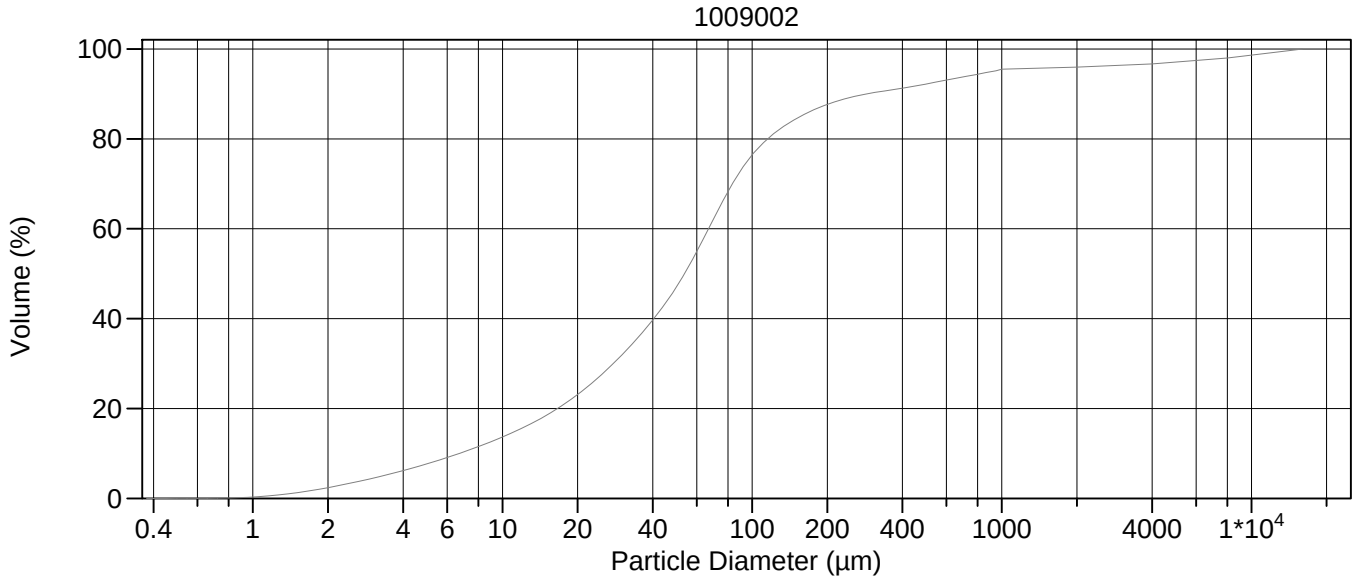

Volume Statistics (Arithmetic) 2a.$02

Calculations from 0.375 µm to 16000 µm

Volume	100.0%		
Mean:	412.8 µm	95% Conf. Limits:	0-3761 µm
Median:	53.61 µm	S.D.:	1708 µm
D(3,2):	16.01 µm	Variance:	2917486 µm^2
Mean/Median Ratio:	7.700	C.V.:	414%
Mode:	66.44 µm	Skewness:	5.620 Right skewed
d_{10}:	6.709 µm	Kurtosis:	31.55 Leptokurtic
d_{50}:	53.61 µm		
d_{90}:	286.7 µm		
Specific Surf. Area	3747 cm^2/ml		

% <	10	25	50	75	90
Size µm	6.709	22.07	53.61	95.70	286.7

2a.$02

Particle Diameter µm	Volume % <	Particle Diameter µm	Volume % <
1.000	0.30	500.0	92.2
2.000	2.40	1000	95.5
5.000	7.72	2000	96.0
10.00	13.7	4000	96.7
15.00	18.5	8000	98.0
20.00	23.1		
50.00	47.2		
60.00	54.9		
63.00	57.2		
70.00	62.2		
75.00	65.4		
90.00	72.9		
125.0	81.6		
200.0	87.7		
250.0	89.3		
400.0	91.3		

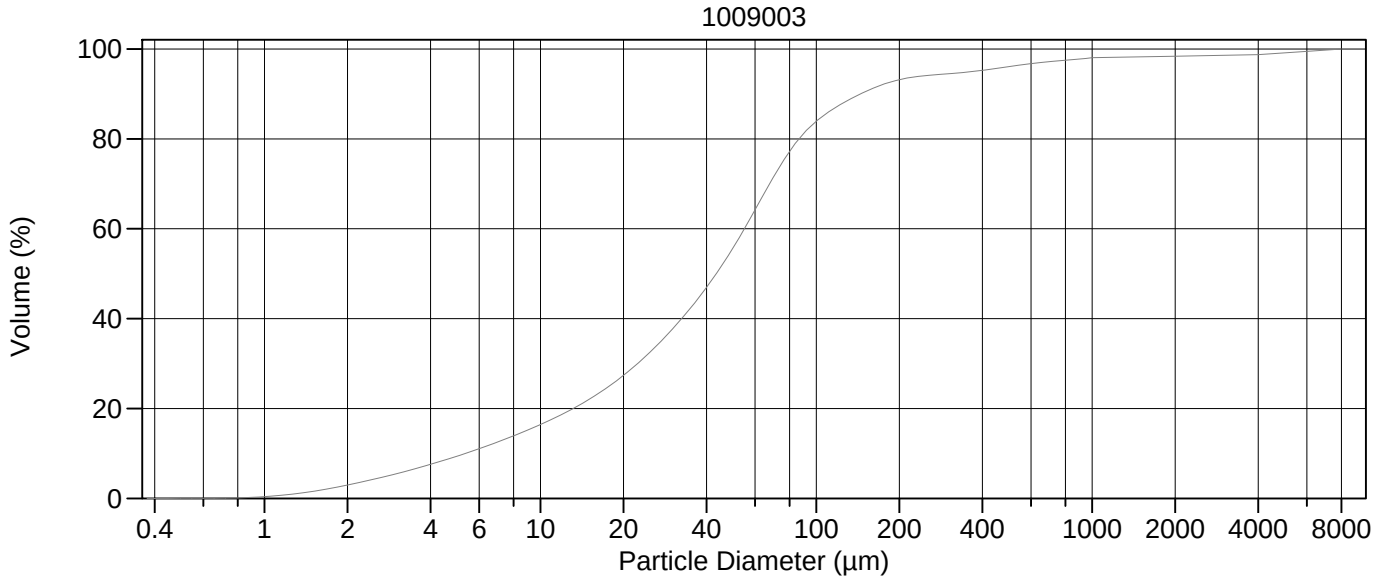

Volume Statistics (Arithmetic) 3a.$02

Calculations from 0.375 µm to 8000 µm

Volume	100.0%		
Mean:	153.4 µm	95% Conf. Limits:	0-1440 µm
Median:	43.42 µm	S.D.:	656.6 µm
D(3,2):	13.51 µm	Variance:	431126 µm^2
Mean/Median Ratio:	3.533	C.V.:	428%
Mode:	60.52 µm	Skewness:	7.688 Right skewed
d_{10}:	5.346 µm	Kurtosis:	60.21 Leptokurtic
d_{50}:	43.42 µm		
d_{90}:	144.7 µm		
Specific Surf. Area	4440 cm^2/ml		

% <	10	25	50	75	90
Size µm	5.346	17.78	43.42	75.71	144.7

3a.$02

Particle Diameter µm	Volume % <	Particle Diameter µm	Volume % <
1.000	0.38	500.0	96.1
2.000	2.98	1000	98.1
5.000	9.41	2000	98.4
10.00	16.4	4000	98.7
15.00	22.0	8000	100
20.00	27.4		
50.00	55.8		
60.00	64.2		
63.00	66.6		
70.00	71.6		
75.00	74.6		
90.00	81.1		
125.0	88.0		
200.0	93.2		
250.0	94.1		
400.0	95.3		

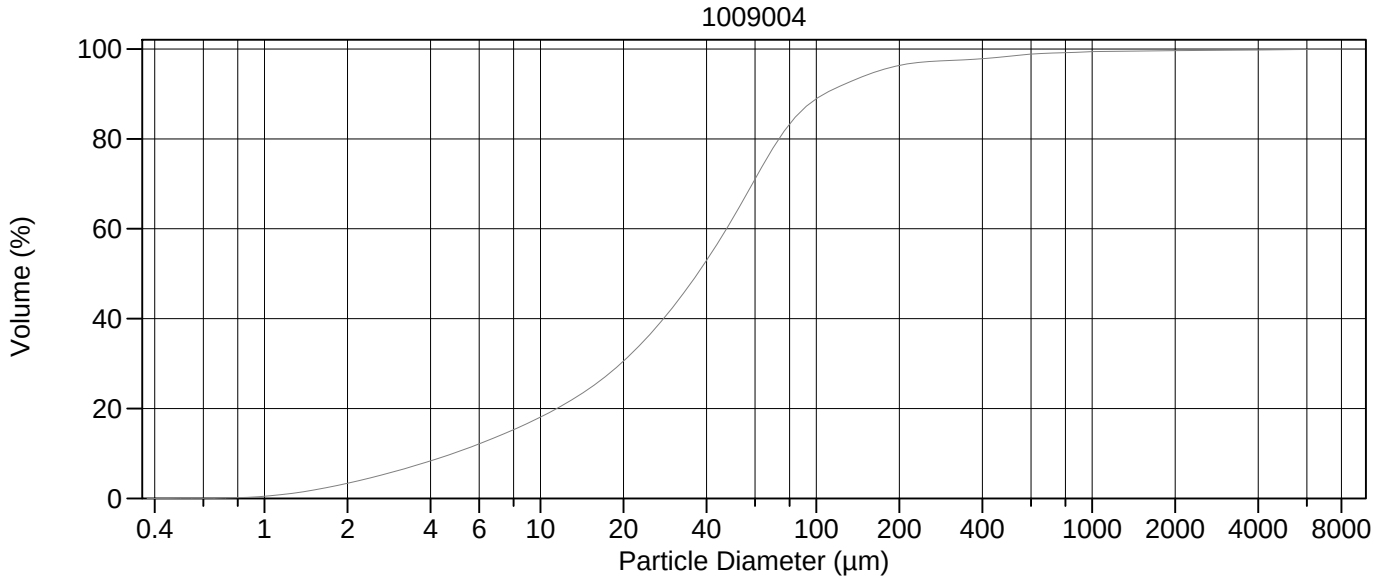

Volume Statistics (Arithmetic) 4a.$02

Calculations from 0.375 µm to 8000 µm

Volume	100.0%		
Mean:	74.80 µm	95% Conf. Limits:	0-666.0 µm
Median:	37.13 µm	S.D.:	301.6 µm
D(3,2):	12.22 µm	Variance:	90988 µm^2
Mean/Median Ratio:	2.014	C.V.:	403%
Mode:	60.52 µm	Skewness:	15.36 Right skewed
d_{10}:	4.822 µm	Kurtosis:	266.4 Leptokurtic
d_{50}:	37.13 µm		
d_{90}:	107.2 µm		
Specific Surf. Area	4911 cm^2/ml		

% <	10	25	50	75	90
Size µm	4.822	15.49	37.13	65.28	107.2

4a.$02

Particle Diameter µm	Volume % <	Particle Diameter µm	Volume % <
1.000	0.49	500.0	98.4
2.000	3.38	1000	99.4
5.000	10.3	2000	99.6
10.00	18.1	4000	99.8
15.00	24.4	8000	100
20.00	30.5		
50.00	62.5		
60.00	71.0		
63.00	73.4		
70.00	78.2		
75.00	80.9		
90.00	86.7		
125.0	92.0		
200.0	96.3		
250.0	97.1		
400.0	97.9		

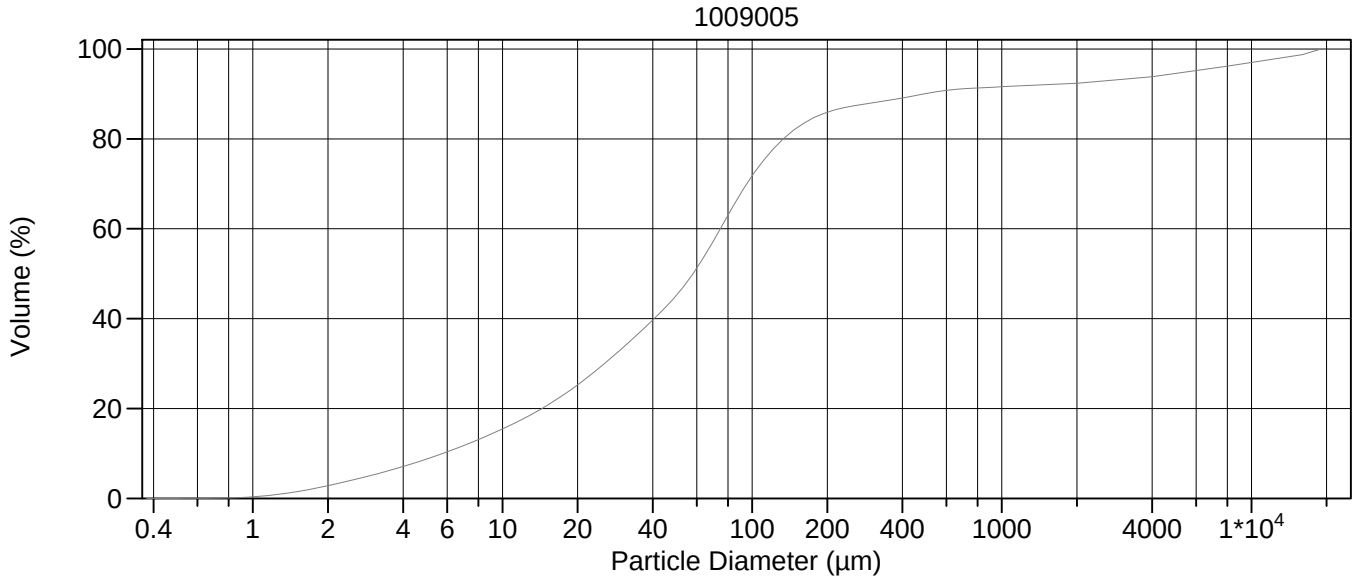

Volume Statistics (Arithmetic) 5a.$02

Calculations from 0.375 µm to 19000 µm

Volume	100.0%		
Mean:	764.8 µm	95% Conf. Limits:	0-6107 µm
Median:	57.98 µm	S.D.:	2726 µm
D(3,2):	14.77 µm	Variance:	7428985 µm^2
Mean/Median Ratio:	13.19	C.V.:	356%
Mode:	72.95 µm	Skewness:	4.499 Right skewed
d_{10}:	5.754 µm	Kurtosis:	20.65 Leptokurtic
d_{50}:	57.98 µm		
d_{90}:	487.2 µm		
Specific Surf. Area	4061 cm^2/ml		

% <	10	25	50	75	90
Size µm	5.754	19.70	57.98	110.3	487.2

5a.$02

Particle Diameter µm	Volume % <	Particle Diameter µm	Volume % <
1.000	0.35	500.0	90.1
2.000	2.84	1000	91.6
5.000	8.82	2000	92.4
10.00	15.5	4000	93.8
15.00	20.6	8000	96.2
20.00	25.3	16000	98.7
50.00	45.3	19000	100
60.00	51.2		
63.00	53.1		
70.00	57.3		
75.00	60.2		
90.00	67.8		
125.0	78.4		
200.0	85.9		
250.0	87.3		
400.0	89.1		

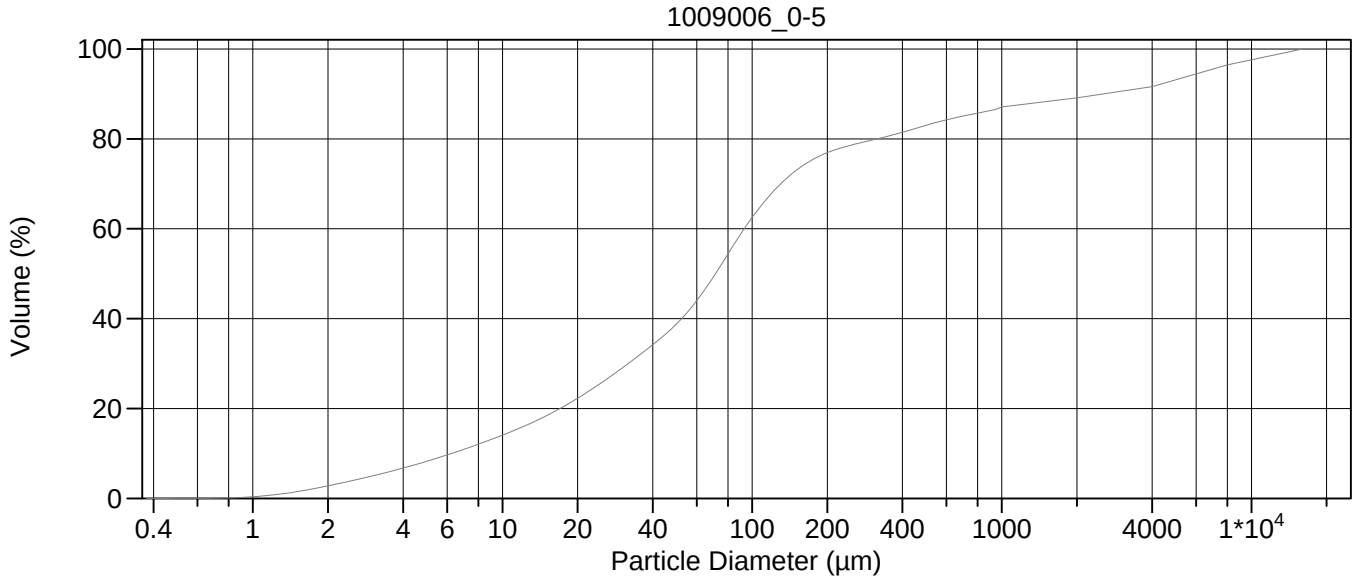

Volume Statistics (Arithmetic) 6a.$02

Calculations from 0.375 µm to 16000 µm

Volume	100.0%		
Mean:	865.7 µm	95% Conf. Limits:	0-5498 µm
Median:	71.31 µm	S.D.:	2363 µm
D(3,2):	16.03 µm	Variance:	5585631 µm^2
Mean/Median Ratio:	12.14	C.V.:	273%
Mode:	5657 µm	Skewness:	3.429 Right skewed
d_{10}:	6.249 µm	Kurtosis:	11.29 Leptokurtic
d_{50}:	71.31 µm		
d_{90}:	2691 µm		
Specific Surf. Area	3742 cm^2/ml		

% <	10	25	50	75	90
Size µm	6.249	23.84	71.31	170.1	2691

6a.$02

Particle Diameter µm	Volume % <	Particle Diameter µm	Volume % <
1.000	0.37	500.0	83.0
2.000	2.79	1000	87.1
5.000	8.29	2000	89.1
10.00	14.1	4000	91.6
15.00	18.4	8000	96.5
20.00	22.3		
50.00	38.9		
60.00	44.0		
63.00	45.6		
70.00	49.3		
75.00	51.9		
90.00	58.8		
125.0	69.0		
200.0	76.9		
250.0	78.6		
400.0	81.5		

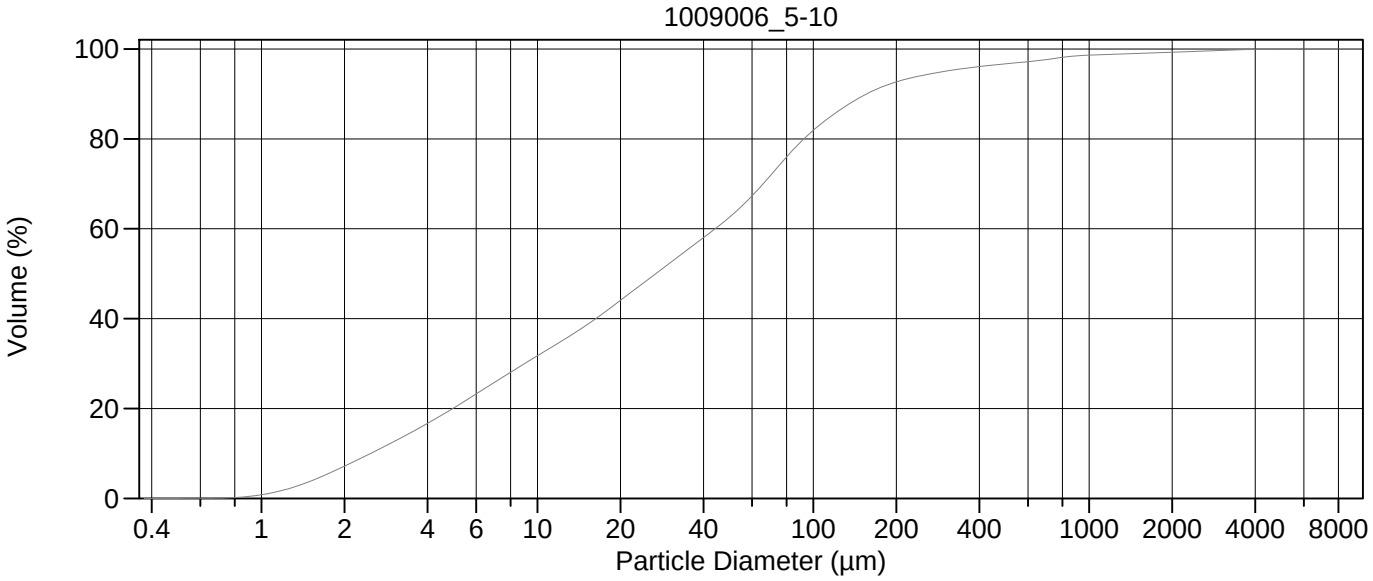

Volume Statistics (Arithmetic) 7#a.$02

Calculations from 0.375 µm to 8000 µm

Volume	100.0%		
Mean:	94.32 µm	95% Conf. Limits:	0-683.1 µm
Median:	26.87 µm	S.D.:	300.4 µm
D(3,2):	7.700 µm	Variance:	90242 µm^2
Mean/Median Ratio:	3.511	C.V.:	318%
Mode:	72.95 µm	Skewness:	8.901 Right skewed
d_{10}:	2.484 µm	Kurtosis:	104.0 Leptokurtic
d_{50}:	26.87 µm		
d_{90}:	156.3 µm		
Specific Surf. Area	7792 cm^2/ml		

% <	10	25	50	75	90
Size µm	2.484	6.665	26.87	77.47	156.3

7#a.$02

Particle Diameter µm	Volume % <	Particle Diameter µm	Volume % <
1.000	0.81	500.0	96.7
2.000	7.19	1000	98.6
5.000	20.2	2000	99.3
10.00	31.7	4000	99.9
15.00	38.5	8000	100
20.00	44.0	16000	100
50.00	62.7		
60.00	67.3		
63.00	68.7		
70.00	71.9		
75.00	74.0		
90.00	79.3		
125.0	86.4		
200.0	92.7		
250.0	94.2		
400.0	96.1		

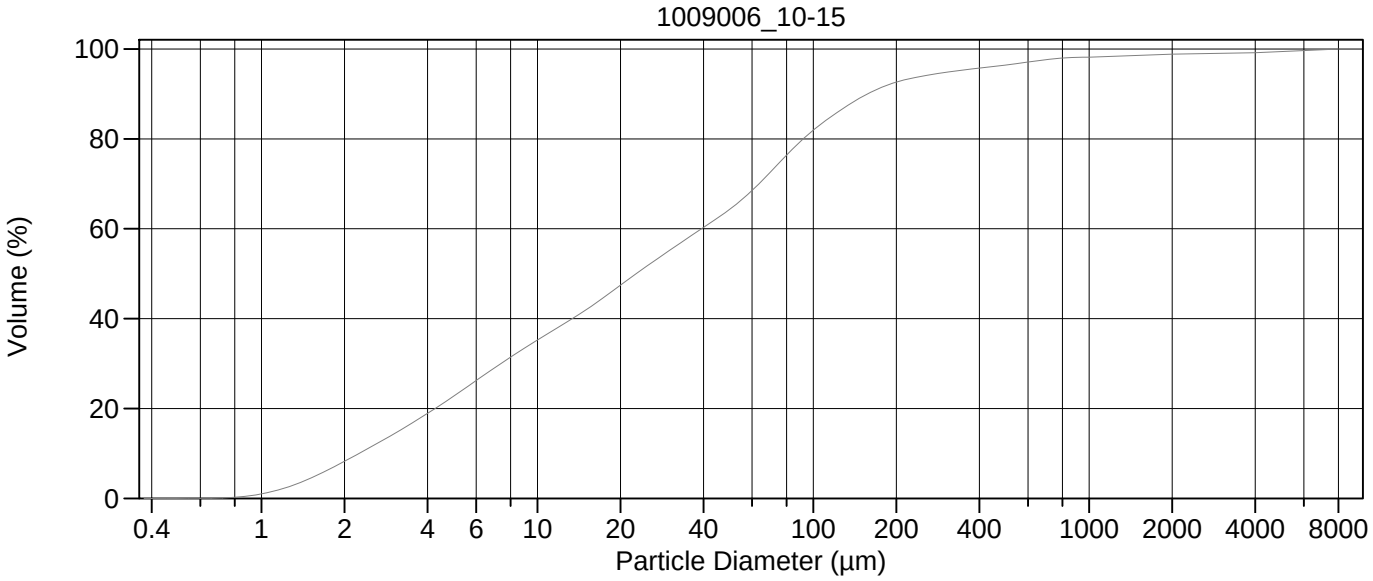

Volume Statistics (Arithmetic) 8a.$02

Calculations from 0.375 µm to 8000 µm

Volume	100.0%		
Mean:	124.6 µm	95% Conf. Limits:	0-1207 µm
Median:	22.81 µm	S.D.:	552.2 µm
D(3,2):	6.949 µm	Variance:	304874 µm^2
Mean/Median Ratio:	5.462	C.V.:	443%
Mode:	72.95 µm	Skewness:	8.891 Right skewed
d_{10}:	2.258 µm	Kurtosis:	83.55 Leptokurtic
d_{50}:	22.81 µm		
d_{90}:	157.4 µm		
Specific Surf. Area	8635 cm^2/ml		

% <	10	25	50	75	90
Size µm	2.258	5.616	22.81	76.09	157.4

8a.$02

Particle Diameter µm	Volume % <	Particle Diameter µm	Volume % <
1.000	1.01	500.0	96.5
2.000	8.26	1000	98.2
5.000	22.9	2000	98.9
10.00	35.2	4000	99.2
15.00	41.9	8000	100
20.00	47.4	16000	100
50.00	64.4		
60.00	68.5		
63.00	69.8		
70.00	72.6		
75.00	74.6		
90.00	79.4		
125.0	86.3		
200.0	92.6		
250.0	94.0		
400.0	95.7		

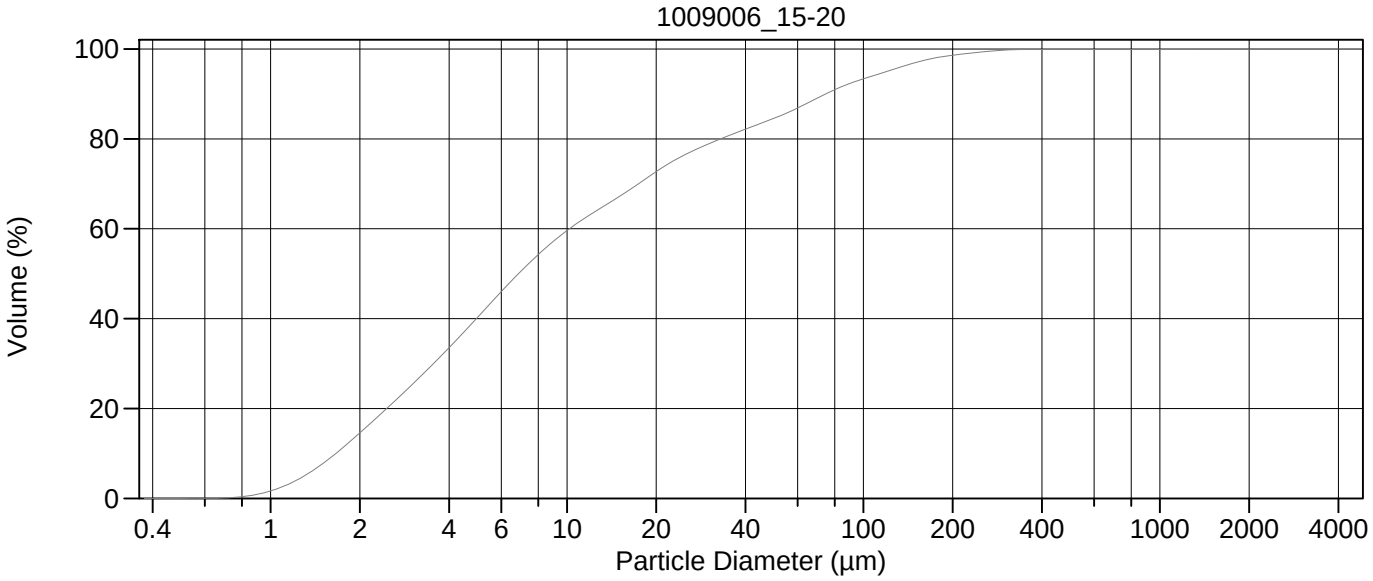

Volume Statistics (Arithmetic) 9a.$02

Calculations from 0.375 µm to 4000 µm

Volume	100.0%		
Mean:	26.70 µm	95% Conf. Limits:	0-180.6 µm
Median:	6.858 µm	S.D.:	78.54 µm
D(3,2):	4.274 µm	Variance:	6168 µm^2
Mean/Median Ratio:	3.892	C.V.:	294%
Mode:	5.355 µm	Skewness:	21.97 Right skewed
d_{10}:	1.661 µm	Kurtosis:	704.6 Leptokurtic
d_{50}:	6.858 µm		
d_{90}:	74.65 µm		
Specific Surf. Area	14040 cm^2/ml		

% <	10	25	50	75	90
Size µm	1.661	2.970	6.858	22.70	74.65

9a.$02

Particle Diameter µm	Volume % <	Particle Diameter µm	Volume % <
1.000	1.67	500.0	99.9
2.000	14.6	1000	99.9
5.000	40.3	2000	100.0
10.00	59.6	4000	100
15.00	67.1	8000	100
20.00	72.7	16000	100
50.00	84.6		
60.00	86.9		
63.00	87.6		
70.00	89.1		
75.00	90.1		
90.00	92.3		
125.0	95.4		
200.0	98.6		
250.0	99.3		
400.0	99.9		

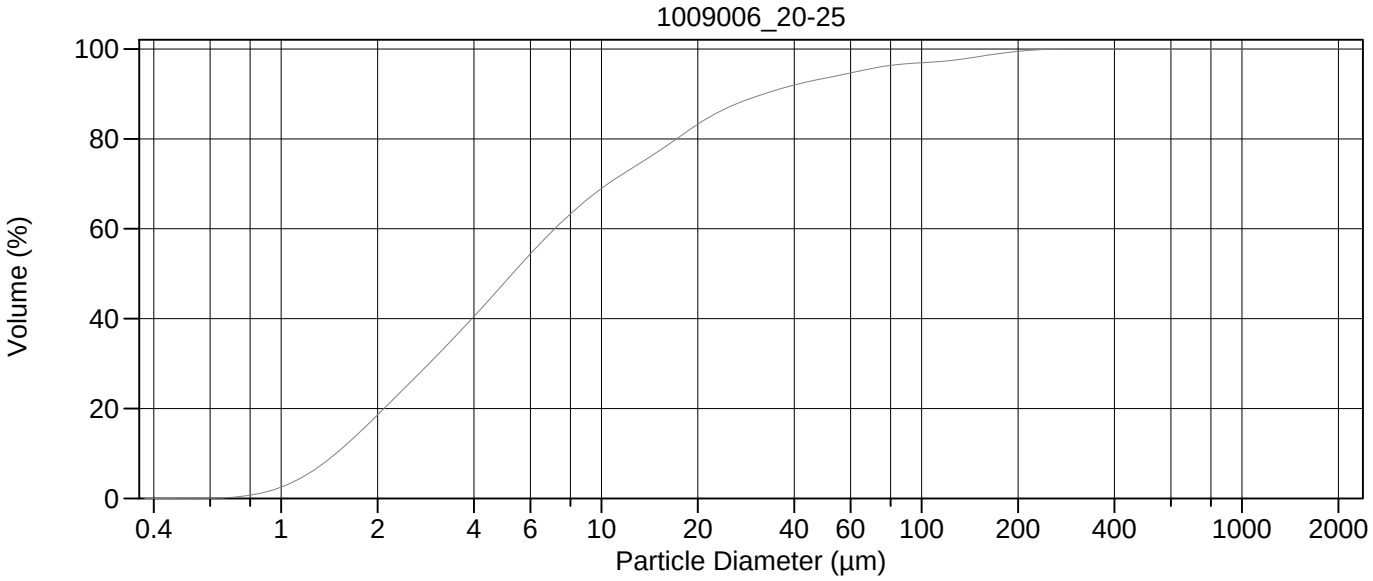

Volume Statistics (Arithmetic) 10.$02

Calculations from 0.375 µm to 2000 µm

Volume	100.0%		
Mean:	15.08 µm	95% Conf. Limits:	0-74.54 µm
Median:	5.281 µm	S.D.:	30.33 µm
D(3,2):	3.557 µm	Variance:	920.0 µm^2
Mean/Median Ratio:	2.856	C.V.:	201%
Mode:	4.878 µm	Skewness:	4.386 Right skewed
d_{10}:	1.485 µm	Kurtosis:	21.96 Leptokurtic
d_{50}:	5.281 µm		
d_{90}:	32.13 µm		
Specific Surf. Area	16867 cm^2/ml		

% <	10	25	50	75	90
Size µm	1.485	2.465	5.281	13.49	32.13

10.$02

Particle Diameter µm	Volume % <	Particle Diameter µm	Volume % <
1.000	2.53	500.0	100
2.000	18.6	1000	100
5.000	48.1	2000	100
10.00	68.9	4000	100
15.00	77.1	8000	100
20.00	83.3	16000	100
50.00	93.5		
60.00	94.7		
63.00	95.0		
70.00	95.7		
75.00	96.1		
90.00	96.7		
125.0	97.5		
200.0	99.5		
250.0	99.9		
400.0	100		

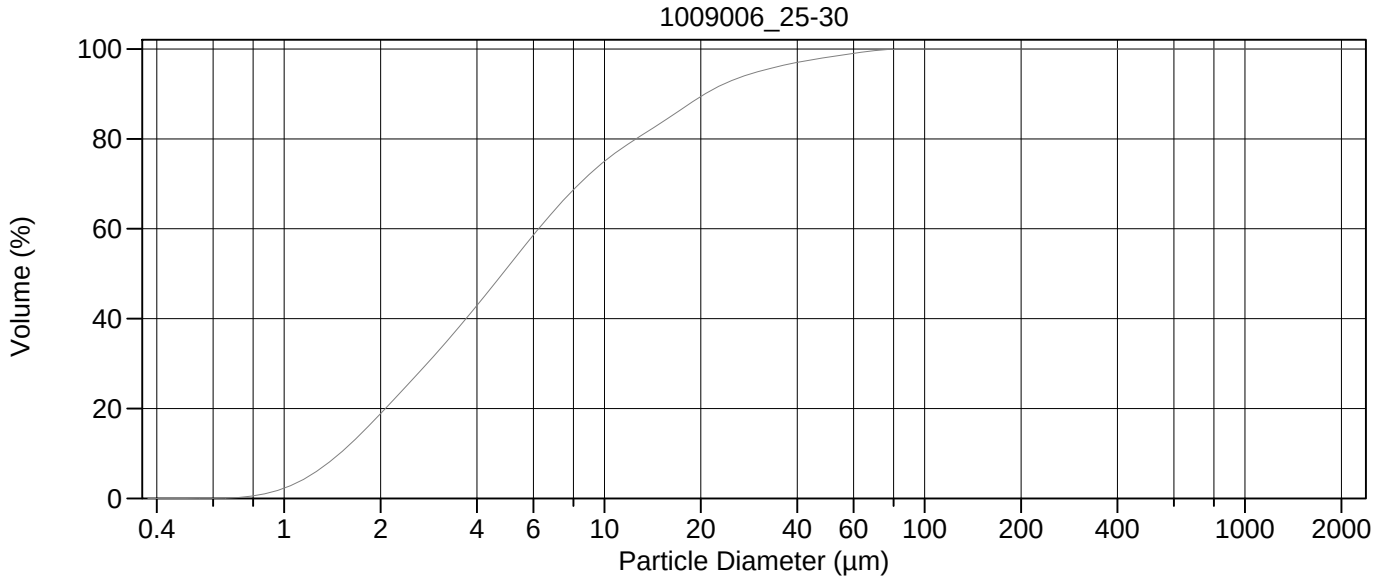

Volume Statistics (Arithmetic) 11.$02

Calculations from 0.375 µm to 2000 µm

Volume	100.0%		
Mean:	8.766 µm	95% Conf. Limits:	0-30.46 µm
Median:	4.812 µm	S.D.:	11.07 µm
D(3,2):	3.402 µm	Variance:	122.6 µm^2
Mean/Median Ratio:	1.822	C.V.:	126%
Mode:	4.878 µm	Skewness:	2.989 Right skewed
d_{10}:	1.492 µm	Kurtosis:	10.95 Leptokurtic
d_{50}:	4.812 µm		
d_{90}:	20.60 µm		
Specific Surf. Area	17634 cm^2/ml		

% <	10	25	50	75	90
Size µm	1.492	2.409	4.812	10.01	20.60

11.$02

Particle Diameter µm	Volume % <	Particle Diameter µm	Volume % <
1.000	2.31	500.0	100
2.000	18.9	1000	100
5.000	51.5	2000	100
10.00	75.0	4000	100
15.00	83.5	8000	100
20.00	89.4	16000	100
50.00	98.2		
60.00	99.0		
63.00	99.2		
70.00	99.6		
75.00	99.8		
90.00	100.0		
125.0	100		
200.0	100		
250.0	100		
400.0	100		

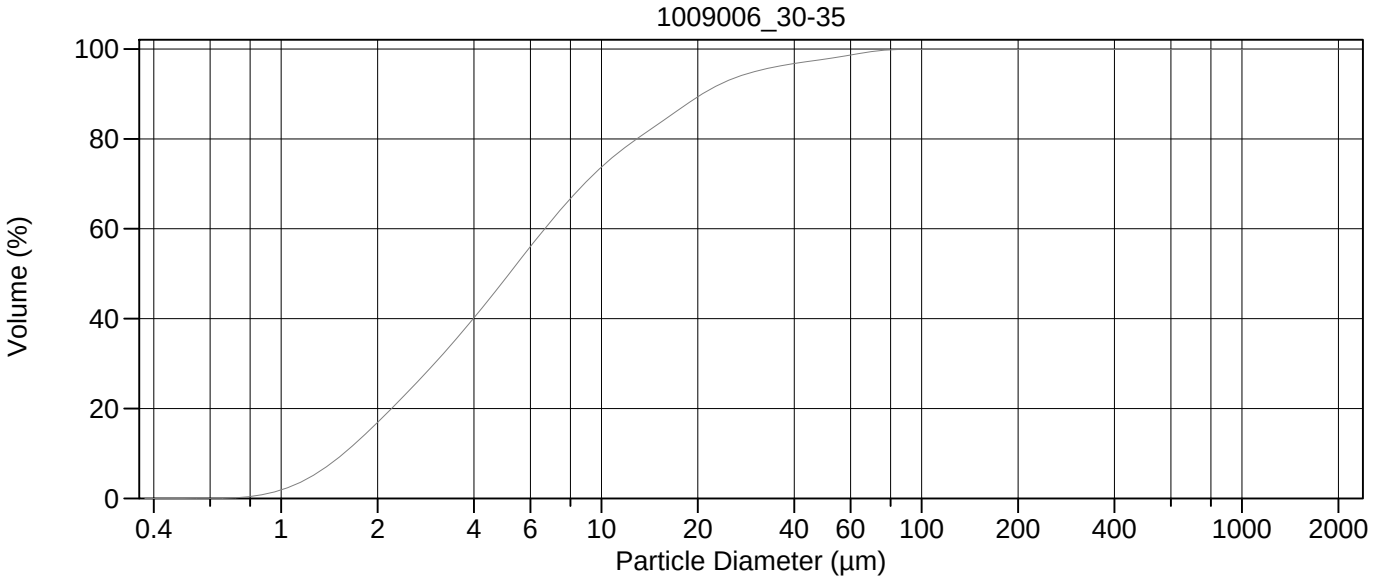

Volume Statistics (Arithmetic) 12a.$02

Calculations from 0.375 µm to 2000 µm

Volume	100.0%		
Mean:	10.06 µm	95% Conf. Limits:	0-86.25 µm
Median:	5.156 µm	S.D.:	38.87 µm
D(3,2):	3.601 µm	Variance:	1511 µm^2
Mean/Median Ratio:	1.952	C.V.:	386%
Mode:	5.355 µm	Skewness:	33.07 Right skewed
d_{10}:	1.569 µm	Kurtosis:	1189 Leptokurtic
d_{50}:	5.156 µm		
d_{90}:	20.66 µm		
Specific Surf. Area	16664 cm^2/ml		

% <	10	25	50	75	90
Size µm	1.569	2.589	5.156	10.49	20.66

12a.$02

Particle Diameter µm	Volume % <	Particle Diameter µm	Volume % <
1.000	1.89	500.0	99.9
2.000	16.9	1000	99.9
5.000	48.8	2000	100
10.00	73.7	4000	100
15.00	83.2	8000	100
20.00	89.3	16000	100
50.00	97.8		
60.00	98.7		
63.00	98.9		
70.00	99.4		
75.00	99.7		
90.00	99.9		
125.0	99.9		
200.0	99.9		
250.0	99.9		
400.0	99.9		

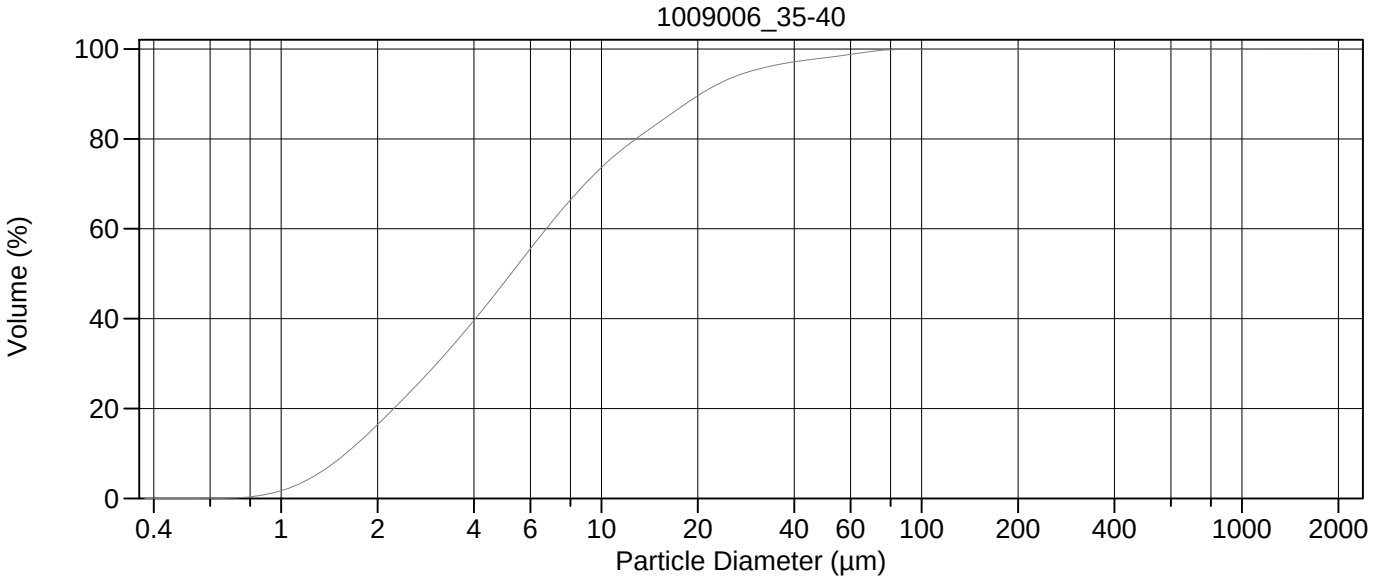

Volume Statistics (Arithmetic) 13a.$02

Calculations from 0.375 µm to 2000 µm

Volume	100.0%		
Mean:	9.947 µm	95% Conf. Limits:	0-85.91 µm
Median:	5.226 µm	S.D.:	38.76 µm
D(3,2):	3.652 µm	Variance:	1502 µm^2
Mean/Median Ratio:	1.904	C.V.:	390%
Mode:	5.355 µm	Skewness:	33.36 Right skewed
d_{10}:	1.593 µm	Kurtosis:	1204 Leptokurtic
d_{50}:	5.226 µm		
d_{90}:	20.39 µm		
Specific Surf. Area	16429 cm^2/ml		

% <	10	25	50	75	90
Size µm	1.593	2.634	5.226	10.50	20.39

13a.$02

Particle Diameter µm	Volume % <	Particle Diameter µm	Volume % <
1.000	1.72	500.0	99.9
2.000	16.4	1000	99.9
5.000	48.2	2000	100
10.00	73.6	4000	100
15.00	83.5	8000	100
20.00	89.6	16000	100
50.00	98.0		
60.00	98.8		
63.00	99.0		
70.00	99.5		
75.00	99.7		
90.00	99.9		
125.0	99.9		
200.0	99.9		
250.0	99.9		
400.0	99.9		

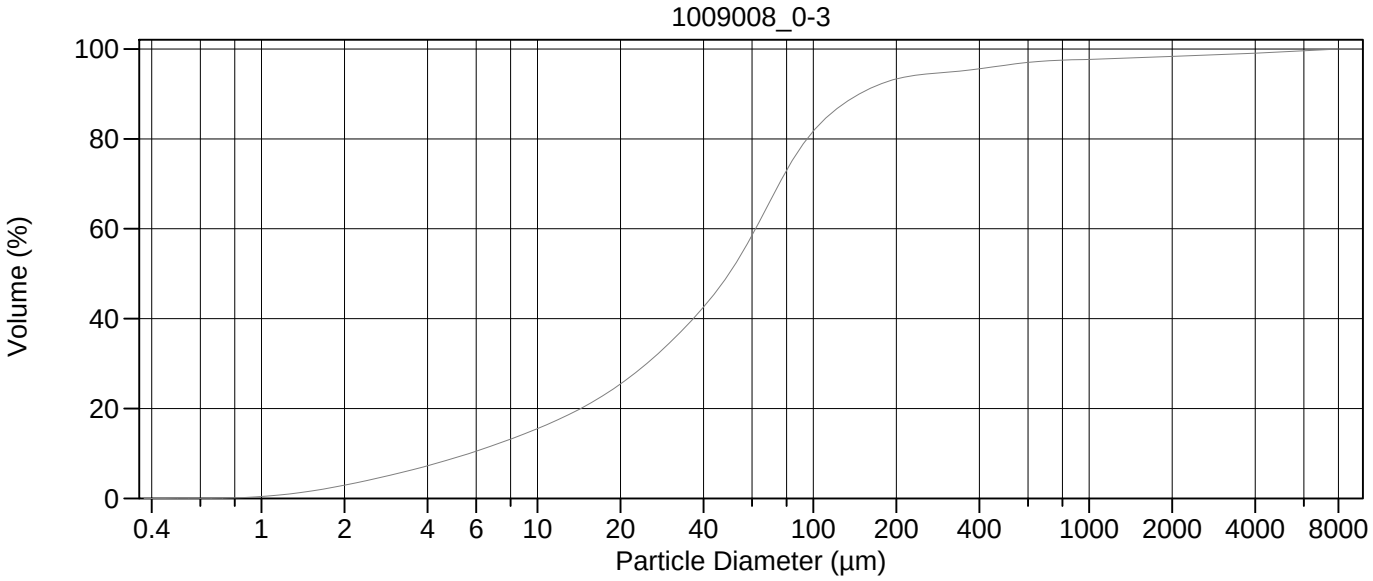

Volume Statistics (Arithmetic) 14a.$02

Calculations from 0.375 µm to 8000 µm

Volume	100.0%		
Mean:	148.7 µm	95% Conf. Limits:	0-1320 µm
Median:	49.50 µm	S.D.:	597.5 µm
D(3,2):	14.09 µm	Variance:	356952 µm^2
Mean/Median Ratio:	3.005	C.V.:	402%
Mode:	66.44 µm	Skewness:	7.935 Right skewed
d_{10}:	5.656 µm	Kurtosis:	66.56 Leptokurtic
d_{50}:	49.50 µm		
d_{90}:	146.9 µm		
Specific Surf. Area	4257 cm^2/ml		

% <	10	25	50	75	90
Size µm	5.656	19.52	49.50	83.62	146.9

14a.$02

Particle Diameter µm	Volume % <	Particle Diameter µm	Volume % <
1.000	0.42	500.0	96.4
2.000	2.96	1000	97.7
5.000	8.97	2000	98.3
10.00	15.5	4000	99.1
15.00	20.6	8000	100
20.00	25.5	16000	100
50.00	50.4		
60.00	58.5		
63.00	61.0		
70.00	66.4		
75.00	69.8		
90.00	78.0		
125.0	87.2		
200.0	93.3		
250.0	94.3		
400.0	95.6		

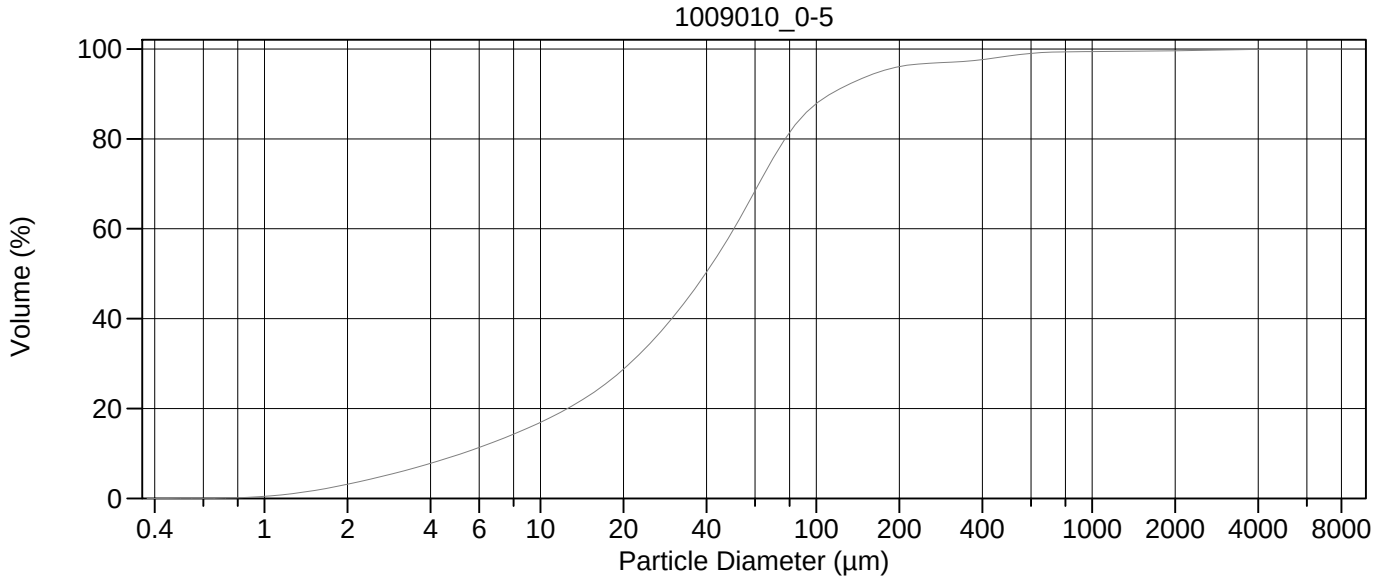

Volume Statistics (Arithmetic) 15#a.$02

Calculations from 0.375 µm to 8000 µm

Volume	100.0%		
Mean:	73.25 µm	95% Conf. Limits:	0-537.9 µm
Median:	39.66 µm	S.D.:	237.1 µm
D(3,2):	12.89 µm	Variance:	56202 µm^2
Mean/Median Ratio:	1.847	C.V.:	324%
Mode:	60.52 µm	Skewness:	14.65 Right skewed
d_{10}:	5.196 µm	Kurtosis:	273.0 Leptokurtic
d_{50}:	39.66 µm		
d_{90}:	112.7 µm		
Specific Surf. Area	4655 cm^2/ml		

% <	10	25	50	75	90
Size µm	5.196	16.81	39.66	68.72	112.7

15#a.$02

Particle Diameter µm	Volume % <	Particle Diameter µm	Volume % <
1.000	0.46	500.0	98.5
2.000	3.16	1000	99.4
5.000	9.66	2000	99.6
10.00	16.9	4000	99.9
15.00	22.9	8000	100
20.00	28.7	16000	100
50.00	59.7		
60.00	68.4		
63.00	70.9		
70.00	75.9		
75.00	78.8		
90.00	85.2		
125.0	91.5		
200.0	96.1		
250.0	96.8		
400.0	97.7		

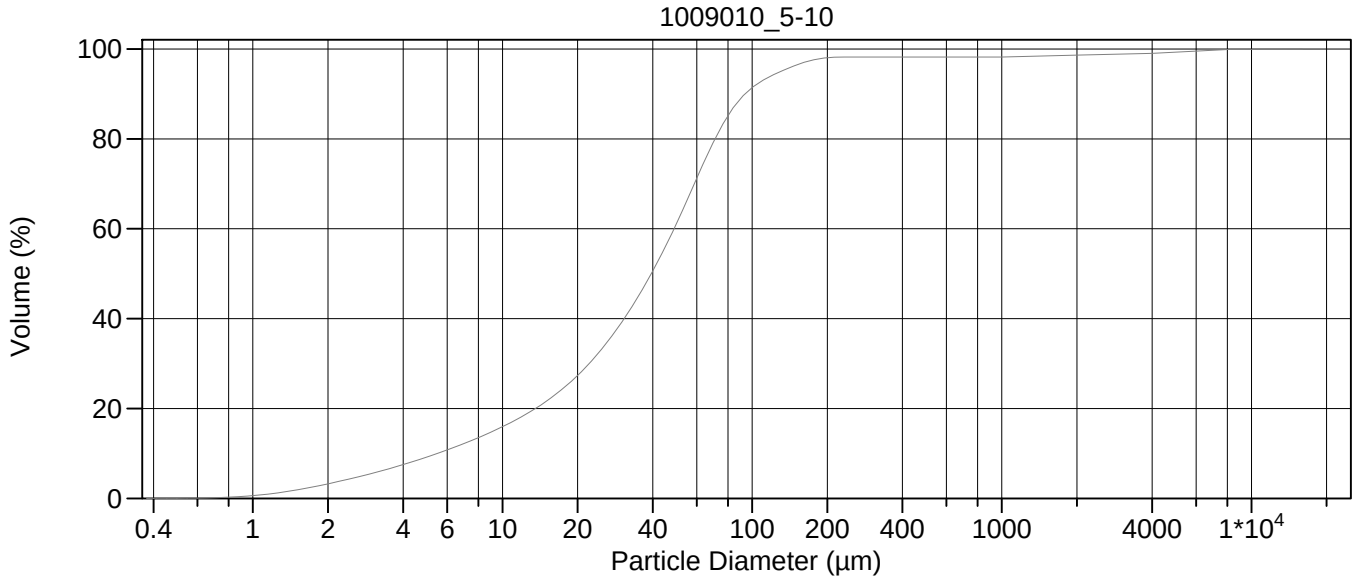

Volume Statistics (Arithmetic) 16#a.$02

Calculations from 0.375 µm to 16000 µm

Volume	100.0%		
Mean:	123.0 µm	95% Conf. Limits:	0-1456 µm
Median:	39.45 µm	S.D.:	680.2 µm
D(3,2):	12.82 µm	Variance:	462676 µm^2
Mean/Median Ratio:	3.118	C.V.:	553%
Mode:	60.52 µm	Skewness:	10.58 Right skewed
d_{10}:	5.494 µm	Kurtosis:	130.1 Leptokurtic
d_{50}:	39.45 µm		
d_{90}:	93.75 µm		
Specific Surf. Area	4680 cm^2/ml		

% <	10	25	50	75	90
Size µm	5.494	17.96	39.45	64.36	93.75

16#a.$02

Particle Diameter µm	Volume % <	Particle Diameter µm	Volume % <
1.000	0.62	500.0	98.2
2.000	3.25	1000	98.2
5.000	9.22	2000	98.6
10.00	16.0	4000	99.0
15.00	21.6	8000	99.9
20.00	27.4	16000	100
50.00	61.4		
60.00	71.2		
63.00	73.9		
70.00	79.3		
75.00	82.5		
90.00	88.9		
125.0	94.6		
200.0	98.0		
250.0	98.2		
400.0	98.2		